Diffusion-based studies on the self-stacking and nanorod formation of platinum(II) intercalators†

Anwen M. Krause-Heuer, Nial J. Wheate,‡ William S. Price and Janice Aldrich-Wright*

Pulsed gradient spin-echo nuclear magnetic resonance diffusion measurements have been used to show that platinum(II)-based intercalating agents self-stack in solution and form nanorods 0.45–3.9 nm in length (at 25 mM); their lengths are dependent on metal complex concentration, salt concentration and solution temperature.

The anticancer agent **56MESS** [(5,6-dimethyl-1,10-phenanthroline)(1S,2S-diaminocyclohexane)platinum(II))]$^{2+}$, Fig. 1a, is our lead candidate in a family of over 60 platinum(II)-based DNA intercalating complexes.[1–4] It has demonstrated significant *in vitro* cytotoxicity in cisplatin sensitive and resistant human cancer cell lines.[5] **56MESS** is thought to induce cellular apoptosis by intercalating double-stranded DNA, thereby preventing DNA transcription and replication.[1] Drug transport, cellular uptake and intracellular glutathione degradation[6] are also thought to play a significant role in the structure–activity relationship of this family of platinum complexes.[1]

A number of new platinum(II)-based DNA intercalator complexes are also being developed that contain terpyridine intercalating groups (*e.g.* [(2,2′:6′,2″-terpyridine)chloro-platinum(II)]$^+$ [Pt(terpy)Cl]$^+$; Fig. 1b).[7–9] A number of these compounds display activity similar to, or greater than, cisplatin in several cell lines.[10]

It is widely accepted that compounds that contain fused aromatic rings are capable of forming dimers in solution through favourable π–π stacking.[11] Platinum(II) complexes containing planar aromatic ligands have been shown to stack and form dimers in aqueous solvents; however, these investigations have been limited to one-dimensional ^{1}H nuclear magnetic resonance (NMR) and electronic spectroscopy.[11–14] The formation of higher order aggregates (*i.e.* greater than two molecules) of these compounds has not been well demonstrated. The self-assembly of these complexes, particularly under physiological-like conditions, is of great importance, as aggregation may influence the ability of the complex to intercalate with DNA. In addition, the formation of large aggregates may influence the rate of drug transport/uptake.[15]
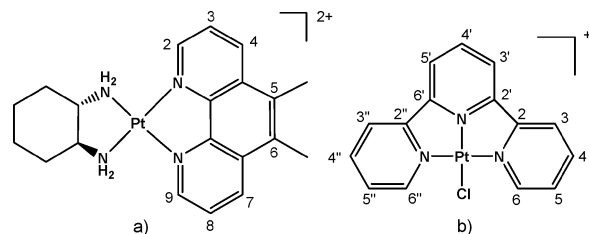
School of Biomedical and Health Sciences, University of Western Sydney, Locked Bag 1797, Penrith South DC, 1797, NSW Australia.
E-mail: j.aldrich-wright@uws.edu.au

† Electronic supplementary information (ESI) available: Experimental methods, sample NMR spectra, a sample plot of the signal attenuation (E) *vs.* $\gamma^2 g^2 \delta^2(\Delta - \delta/3)$, calculation of ellipsoid lengths and plots of chemical shift and diffusion coefficient *vs.* metal complex and salt concentrations. See DOI: 10.1039/b820584a

‡ *Present address*: Strathclyde Institute of Pharmacy and Biomedical Sciences, University of Strathclyde, John Arbuthnott Building, 27 Taylor Street, Glasgow, UK G4 0NR.

Fig. 1 The chemical structure of (a) **56MESS** and (b) [Pt(terpy)Cl]$^+$, indicating the numbering system adopted.

56MESS and [Pt(terpy)Cl]$^+$ serve as excellent model compounds for initial investigations of such aggregation mechanisms. Thus, we have studied the self-aggregation of **56MESS** and [Pt(terpy)Cl]$^+$ at varying metal complex/salt concentrations and solution temperatures using pulsed gradient spin-echo (PGSE) NMR diffusion measurements.[16]

X-Ray crystal structures have shown that platinum(II)-based DNA intercalators can π–π stack in three different configurations; a head-to-head,[17] head-to-tail[18] or pinwheel configuration, where alternate intercalator molecules are rotated ∼90° compared to the molecule stacked above it.[2] In any configuration, the resultant macromolecule forms a cylinder or rod-like structure. We have employed the simple model of an ellipsoid (oblate or prolate, ESI†, Fig. S5) for the determination of macromolecule length. By substituting the observed diffusion coefficient and the translational friction coefficient of an ellipsoid (oblate or prolate) into the Stokes–Einstein equation,[19] we have calculated the length of the nanorod and the estimated number of stacked intercalator molecules each contains (ESI†).

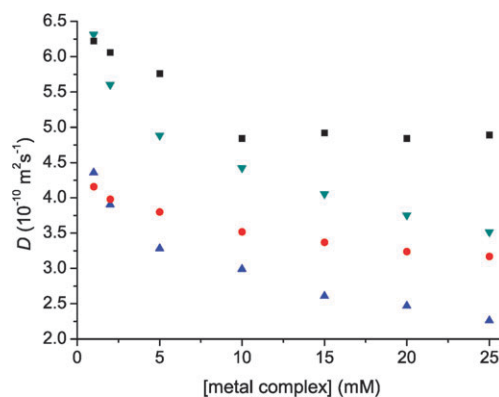The comparison of the chemical shift (ESI†, Fig. S6) to the diffusion coefficient (Fig. 2) of **56MESS** and [Pt(terpy)Cl]$^+$

Fig. 2 The diffusion coefficient of **56MESS** (■ 37 °C, ● 25 °C) and [Pt(terpy)Cl]$^+$ (▼ 37 °C, ▲ 25 °C) with increasing concentration.

Table 1 The diffusion coefficients (*D*; 10^{-10} m^2 s^{-1}) and chemical shifts (ppm) of **56MESS** (methyl resonance) and [Pt(terpy)Cl]$^+$ (H5 resonance) in D$_2$O with increasing metal complex concentration and solution temperature. Errors are given in brackets

[**56MESS**]/ mM	*D* {25 °C}	δ CH$_3$/ppm {25 °C}	*D* {37 °C}	δ CH$_3$/ppm {37 °C}
1.0	4.16 (0.01)	2.79	6.22 (0.02)	2.81
2.0	3.98 (0.01)	2.79	6.06 (0.02)	2.79
5.0	3.80 (0.01)	2.74	5.76 (0.01)	2.74
10	3.52 (0.02)	2.63	4.84 (0.01)	2.68
15	3.37 (0.01)	2.58	4.90 (0.01)	2.61
20	3.27 (0.01)	2.55	4.84 (0.01)	2.59
25	3.17 (0.01)	2.51	4.89 (0.01)	2.56

[Pt(terpy)Cl]$^+$/ mM	*D* {25 °C}	δ H5/ppm {25 °C}	*D* {37 °C}	δ H5/ppm {37 °C}
1.0	4.36 (0.03)	7.64	6.31 (0.05)	7.81
2.0	3.90 (0.01)	7.58	5.60 (0.01)	7.77
5.0	3.28 (0.01)	7.52	4.89 (0.01)	7.70
10	2.99 (0.01)	7.48	4.42 (0.01)	7.64
15	2.61 (0.01)	7.45	4.06 (0.01)	7.59
20	2.47 (0.01)	7.37	3.76 (0.01)	7.56
25	2.26 (0.01)	7.36	3.52 (0.01)	7.53

demonstrates that chemical shift change alone is not an accurate method for determining the extent of aggregation. The methyl resonance of **56MESS** and the H5 resonance of [Pt(terpy)Cl]$^+$ experience the same magnitude (0.28 ppm) of upfield chemical shift with increasing concentration; however, the reduction of the diffusion coefficient differs between the two complexes (Table 1). The diffusion coefficient of **56MESS** is reduced by 1.0×10^{-10} m^2 s^{-1} (24%) and 1.3×10^{-10} m^2 s^{-1} (22%) when the concentration in increased from 1 to 25 mM, at 25 °C and 37 °C, respectively. This is compared to the diffusion coefficient of [Pt(terpy)Cl]$^+$, which is reduced by 2.1×10^{-10} m^2 s^{-1} (25 °C, 48%) and 2.8×10^{-10} m^2 s^{-1} (37 °C, 44%) over the same concentration range.§ In addition, the chemical shift of the methyl resonance at each metal complex concentration is less sensitive to an increase in temperature than the H5 resonance (~ 0.05 ppm compared to ~ 0.19 ppm). These results contrast the differences between using diffusion and chemical shifts for probing the degree of stacking, and show that measurement of chemical shift alone is not a reliable method for determining the extent of aggregation. The diffusion coefficient (Fig. 2) is more sensitive to changes in molecule size due to aggregation, and in combination with the simple ellipsoid model, is a more appropriate and extremely useful method for determining the size of stacks formed.

At 25 °C, the diffusion coefficients of **56MESS** and [Pt(terpy)Cl]$^+$ decrease monotonically with increasing concentration (Fig. 2, Table 1), indicating the formation of larger particles. At the lowest concentration examined (1 mM) the **56MESS** macromolecule contains ~ 2–3 molecules, creating a nanorod that is only 0.6 nm in length. At 25 mM, there are ~ 3–4 molecules in the nanorod, with a length of 1.0 nm (Fig. 3a). [Pt(terpy)Cl]$^+$, however, appears to self-stack to a much greater extent than **56MESS**, with nanorods 0.7–2.9 nm (~ 3–10 molecules) in length formed as the concentration is increased up to 25 mM (Fig. 3b). At high concentrations (15–25 mM) the resonances of [Pt(terpy)Cl]$^+$ also experience
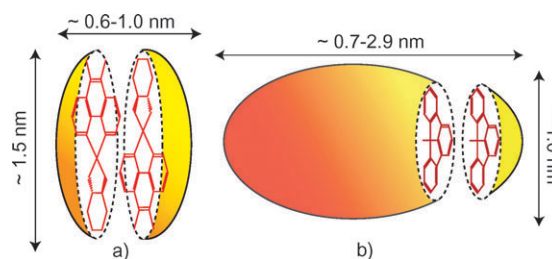

Fig. 3 A schematic representation of the head-to-tail stacking at 25 °C of (a) the oblate (disk-like) model of **56MESS** and (b) the prolate (rod-like) model of [Pt(terpy)Cl]$^+$ (no NaCl present).

a greater degree of broadening, supporting this finding of aggregation.

The aggregation of both complexes was also examined at a higher temperature (37 °C).¶ The higher temperature reduces the size of the aggregates formed; at the lowest concentration (1 mM) **56MESS** does not appear to undergo stacking. Between 2 and 10 mM the reduction in the diffusion coefficient suggests that some stacking does occur; however, it does not change between 10 and 25 mM (Table 1), with the maximum nanorod formed consisting of ~ 2–3 molecules, with length 0.5 nm. [Pt(terpy)Cl]$^+$ does not appear to have the same upper limit on the size of the nanorod formed, with the diffusion coefficient continuing to decrease with increasing concentration (up to 25 mM). The nanorods formed are also longer than those of **56MESS**, consisting of a maximum of ~ 4–5 molecules, with a length of 1.2 nm. These results may have implications in the delivery and transport of DNA intercalating drugs, particularly platinum(II)-based drugs, in disease treatment.

The effect of salt concentration on nanorod formation was also investigated, as the concentration of salt (NaCl) is between 4 and 20 mM inside cells and as high as 155 mM in intravenous drug infusions.[20] Various experimental conditions such as ionic strength,[11,12] pH[12] and counter-ion[14] have been shown to influence the self-assembly of platinum(II) inter-calators. The incorporation of metal ions into solid-state structures of platinum complexes has been shown to stabilise the stacking of the molecules into columns.[18] Conversely, it has been shown that the addition of alkali metal salts (especially NaCl) decreases the viscosity of D$_2$O and H$_2$O,[21,22] which disrupts the hydrogen bonding between water molecules, allowing solutes to diffuse faster through solution. Under our experimental conditions, it appears that varying

Table 2 The diffusion coefficients (*D*; 10^{-10} m^2 s^{-1}) and chemical shifts (ppm) of **56MESS** and [Pt(terpy)Cl]$^+$ (20 mM, D$_2$O, 25 °C) at increasing concentrations of NaCl. Errors are given in brackets

NaCl/mM	*D* **56MESS**	δ CH$_3$/ppm	*D* [Pt(terpy)Cl]$^+$	δ H5/ppm
0.0	3.27 (0.01)	2.55	2.47 (0.01)	7.37
2.0	3.26 (0.01)	2.55	2.40 (0.01)	7.35
5.0	3.26 (0.01)	2.54	2.34 (0.01)	7.34
7.0	3.26 (0.01)	2.54	2.30 (0.01)	7.33
10	3.24 (0.01)	2.53	2.23 (0.01)	7.31
15	3.22 (0.01)	2.52	2.16 (0.01)	7.30
20	3.22 (0.01)	2.52	2.10 (0.01)	7.29
35	3.17 (0.01)	2.49	ND	ND
50	3.11 (0.01)	2.46	ND	ND
65	3.10 (0.01)	2.45	ND	ND

NaCl concentration does not significantly affect the diffusion of **56MESS**, up to 1 : 1 equiv.; however, it does change over a greater concentration range (Table 2, ESI†, Fig. S7). The diffusion coefficient of $[Pt(terpy)Cl]^+$, however, decreases significantly with increasing NaCl concentration (up to 1 : 1 equiv.), with the chemical shift change of the H5 resonance following a similar trend (ESI†, Fig. S8). As $[Pt(terpy)Cl]^+$ diffuses much slower in solutions of higher NaCl concentrations, it indicates there is an additional effect that is more significant than the reduced viscosity of the solvent and may be due to the facilitation of longer stack formation. It was observed that the addition of NaCl to the solutions promoted crystallisation, with the degree and speed of crystallisation proportional to the concentration of NaCl. It is therefore most likely that the addition of NaCl to $[Pt(terpy)Cl]^+$ (20 mM) promotes the self-stacking of the molecules, with the length of the nanorod increasing from ~2.9 nm to 3.9 nm. The mechanism by which NaCl interacts with $[Pt(terpy)Cl]^+$ in the solution-phase is still unclear and is under further investigation.

Despite 40 years of research, the mechanism by which platinum drugs (like cisplatin and carboplatin) are transported into cells is still not clear. Cisplatin complexes are neutrally charged (although they can become slightly cationic (1+ or 2+) upon hydrolysis within the cell) and may only interact weakly with negatively charged cell membranes. Both $[Pt(terpy)Cl]^+$ and **56MESS** nanorods, however, are more cationic (4+ to 12+) at physiological temperature, and so may have stronger electrostatic interactions with cell surfaces. In addition, the nanorods formed by **56MESS** and $[Pt(terpy)Cl]^+$ are of similar diameter to some biomolecules (*e.g.* insulin ~3.0 nm and cytochrome C ~4.0 nm).[23] Tumour vasculature is known to have enhanced permeability to macromolecules,[15] which may have a positive effect on the uptake of **56MESS** in cancerous tissues.

Overall, these results have implications not just in the delivery of platinum-based DNA intercalating agents, but for all small molecule drugs that contain fused aromatic ring systems, such as doxorubicin and daunorubicin, which are routinely used in the treatment of human breast cancers. These results are also extremely relevant in the investigations of bis-intercalating compounds and the interactions of these aggregates with biomolecules. They also highlight the usefulness of PGSE diffusion NMR in the measurement of aggregation of intercalating complexes, which will be the focus of further work.

Notes and references

§ The contribution of viscosity to the diffusion measurements was assessed by measuring the diffusion coefficient of the residual HDO in each experiment. This did not change over the concentration range. In addition, the volume fraction was less than 1% in all experiments.

¶ Convection effects at 37 °C were assessed by measuring the diffusion at different Δ values and were found not to contribute to the apparent diffusion coefficients measured.

1 S. Kemp, N. J. Wheate, D. P. Buck, M. Nikac, G. J. Collins and J. R. Aldrich-Wright, *J. Inorg. Biochem.*, 2007, **101**, 1049–1058.
2 D. M. Fisher, P. J. Bednarski, R. Grunert, P. Turner, R. R. Fenton and J. R. Aldrich-Wright, *ChemMedChem*, 2007, **2**, 488–495.
3 D. Jaramillo, D. P. Buck, J. G. Collins, R. R. Fenton, F. H. Stootman, N. J. Wheate and J. R. Aldrich-Wright, *Eur. J. Inorg. Chem.*, 2006, 839–849.
4 C. R. Brodie, J. G. Collins and J. R. Aldrich-Wright, *Dalton Trans.*, 2004, 1145–1152.
5 N. J. Wheate, R. I. Taleb, A. M. Krause-Heuer, R. L. Cook, S. Wang, V. J. Higgins and J. R. Aldrich-Wright, *Dalton Trans.*, 2007, 5055–5064.
6 S. Kemp, N. J. Wheate, M. J. Pisani and J. R. Aldrich-Wright, *J. Med. Chem.*, 2008, **51**, 2787–2794.
7 G. Lowe, A.-S. Droz, T. Vilaivan, G. W. Waever, J. J. Park, J. M. Pratt, L. Tweedale and L. R. Kelland, *J. Med. Chem.*, 1999, **42**, 3167–3174.
8 G. Lowe, A.-S. Droz, J. J. Park and G. W. Waever, *Bioorg. Chem.*, 1999, **27**, 477–486.
9 G. Lowe, J. A. McCloskey, J. Ni and T. Vilaivan, *Bioorg. Med. Chem.*, 1996, **4**, 1007–1013.
10 K. Becker, C. Herold-Mende, J. J. Park, G. Lowe and R. H. Schirmer, *J. Med. Chem.*, 2001, **44**, 2784–2792.
11 G. Arena, L. Monsú Scolaro, R. F. Pasternack and R. Romeo, *Inorg. Chem.*, 1995, **34**, 2994–3002.
12 C. Yu, K. H.-Y. Chan, K. M.-C. Wong and V. W.-W. Yam, *Chem.–Eur. J.*, 2008, **14**, 4577–4584.
13 V. W.-W. Yam, K. M.-C. Wong and N. Zhu, *J. Am. Chem. Soc.*, 2002, **124**, 6506–6507.
14 V. W.-W. Yam, K. H.-Y. Chan, K. M.-C. Wong and N. Zhu, *Chem.–Eur. J.*, 2005, **11**, 4353–4543.
15 T. W. Hambley, *Aust. J. Chem.*, 2008, **61**, 647–653.
16 P. Stilbs, *Prog. Nucl. Magn. Reson. Spectrosc.*, 1987, **19**, 1.
17 K. W. Jennette, J. T. Gill, J. A. Sadownick and S. J. Lippard, *J. Am. Chem. Soc.*, 1976, **98**, 6159–6168.
18 M. van Holst, D. Le Pevelen and J. R. Aldrich-Wright, *Eur. J. Inorg. Chem.*, 2008, 4608–4615.
19 W. S. Price, *NMR Studies of Translational Motion*, Cambridge University Press, Cambridge, UK, 2009.
20 Y. Jung and S. J. Lippard, *Chem. Rev.*, 2007, **107**, 1387–1407.
21 Z. Hai-Lang and H. Shi-Jun, *J. Chem. Eng. Data*, 1996, **41**, 516–520.
22 A. G. Ostroff, B. S. Snowden, Jr and D. E. Woessner, *J. Phys. Chem.*, 1969, **73**, 2784–2785.
23 R. Esfand and D. A. Tomalia, *Drug Discovery Today*, 2001, **6**, 427–436.